EFFECTS DUE TO GRAVITY AND CURVED SPACE IN STATISTICAL AND QUANTUM MODELS

Andriy Nazarenko

Bogolyubov Institute for Theoretical Physics of NAS of Ukraine

Berlin, March 4, 2025

Outline

Intro

The subject of our research is equations of state and phase diagrams of matter, phase transitions, the role of topology and geometry of space in the evolution of systems, and the effects of the mutual influence of matter and space-time.

In this talk we are focusing on 7 problems (5 with Prof. Gavrilik, and indexed by (year)) in areas 2-4 from the list of our interests:
1. strong interacting matter (nuclear, quark-gluon and partonic systems)
2. models on manifolds (Riemann surfaces, homogeneous spaces, Teichmüller space, complements of links and knots)
3. gravitating systems (extremal black holes, Chern-Simons gravity, general relativity)
4. dark matter models (μ-deformed bosons, Bose-Einstein condensate DM with two-phase structure and two-particle composites)

1. Many-particle systems

1.1 Revealing extra dimensions in the quark-gluon system
1.2 Photon gas with Planck upper bound of energy
1.3 The role of statistics in an ensemble of extremal black holes

1.1 Revealing extra dimensions in the quark-gluon system

In the 2000s, models of microscopic BHs were considered for an arbitrary number d of extra spatial dimensions, which prompted us to find the most probable d.

Assuming (2008) that the 4-dim Universe exists, but in the presence of dense matter (quarks+gluons) with a certain EMT, extra dimensions with the d-torus topology and periodic coordinates $\phi_n \in [0, 2\pi L]$, $n = \overline{1, d}$ may appear. Their size L is resulted from the concept of Arkani-Hamed, Dimopoulos and Dvali (ADD), as for the mBH:

$$M_{\rm f}^{2+d} \int {\rm d}^d\phi = M_{\rm Pl}^2, \text{ and } M_{\rm f} \sim M_{\rm EW} \sim 10^3 \text{ GeV at } d = 2,$$

where $M_{\rm f}$ is new fundamental mass in $4 + d$ dimensions, the Planck mass $M_{\rm Pl}$.

We characterize 3 dimensions by the scale factor a, and d dimensions by $b \leq 1$ in the fireball region $r < r_{\rm fb} \simeq 7$ fm, and formulate Einstein equations in $4 + d$ dimensions with a source (MIT-bag) for the space-time interval

$$ {\rm d}s^2 = -{\rm d}t^2 + a^2(t)({\rm d}x^2 + {\rm d}y^2 + {\rm d}z^2) + b^2(t) \sum_{n=1}^{d} {\rm d}\phi_n^2 .$$

The Hamiltonian constraint gives the quantum Wheeler–DeWitt equation with the potential $W(a) = Ba^3 + CT^4/a$ ($B^{1/4} = 200$ MeV) in terms of $\xi = ab^{d/2}$, $v = b^d$:

$$\left[\xi^2 \frac{\partial^2}{\partial \xi^2} - \frac{12d}{d+2} v^2 \frac{\partial^2}{\partial v^2} + \varkappa^2 \frac{\xi^3}{\sqrt{v}} W\left(\frac{\xi}{\sqrt{v}}\right)\right] \Psi_d = 0,$$

here $\varkappa^2 \equiv 24 M_{\rm Pl}^2 V_{\rm fb}^2 \approx 2.5 \cdot 10^{36}$ MeV^{-4}. It has a correct limit at $d = 0$.

Further, we use the WKB approximation due to the large $\varkappa^2$, and $b = 1$ in $\Psi_{d>0}$.

- Mode of confinement: $B \gg T^4$
  Let matter, with pressure $P < 0$, collapse in 3 dimensions to some $0 < a_0 < 1$ for all d.
  Then, the amplitude of transition "3"→"$3+d$" (using the Kummer function $U(a,b,z)$) is
  $$|\langle 3|3+d\rangle| = \left|1 + \mathrm{i}\mu z U\left(1, \tfrac{5}{3}, -\mathrm{i}\mu z\right)\right|$$
  $$\mu \equiv \varkappa\sqrt{B}a_0^3/3,\ z = \sqrt{1+\tfrac{4d}{6-d}} - 1$$
  Probability density $\mathcal{P}(d)$ for d results in
  1) $d_{\max} = 6$ (as in the string theory);
  2) $\langle d\rangle = 2$ (as in the ADD model) for $\mu \approx 0.11$.

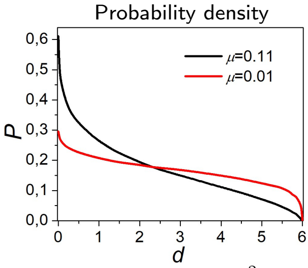

$$\mathcal{P}(d) = \frac{|\langle 3|3+d\rangle|^2}{\int_0^6 |\langle 3|3+x\rangle|^2 \mathrm{d}x}$$

- Mode of radiation dominance: $B \ll T^4$
  In terms of quasi-momentum $k(T) = \varkappa\sqrt{C}T^2$, the amplitude and probability of transition from 3-dim with $k_{\text{in}} = k(T_{\text{in}})$ to $(3+d)$-dim with $k_{\text{fin}} = k(T_{\text{fin}})$:
  $$\langle 3, k_{\text{in}}|3+d, k_{\text{fin}}\rangle = \delta(k_{\text{in}} - k_{\text{fin}}) - \frac{3d}{2(d+2)}\frac{1}{k_{\text{fin}}}\theta(k_{\text{in}} - k_{\text{fin}})$$
  $$\mathrm{Prob}(d) = 1 - \frac{3d}{2(d+2)}\frac{1}{k_{\text{in}}}.$$
  Here, revealing extra dimensions is accompanied by cooling, when $T_{\text{fin}} \le T_{\text{in}}$, and the probability increases with growing initial temperature T_{in} of the matter.

1.2 Photon gas with Planck upper bound of energy

At high energies and temperatures, instead of the addition law $\epsilon_{\rm tot} = \epsilon_1 + \epsilon_2$, we introduce "$\kappa$-addition" $E_{\rm tot} = E_1 \oplus_\kappa E_2$ according to the double special relativity (DSR) and $\kappa \simeq M_{\rm Pl}$ (or $\simeq M_{\rm f}$):

$$a \oplus_\kappa b = \frac{\frac{a}{1-a/\kappa} + \frac{b}{1-b/\kappa}}{1 + \frac{1}{\kappa}\left(\frac{a}{1-a/\kappa} + \frac{b}{1-b/\kappa}\right)}, \quad E \oplus_\kappa \kappa = \kappa.$$

Applying the Planck limit to each mode with frequency $\omega = c|\mathbf{k}|$ and photon number n_ω in volume V (2019), the partition function is written as

$$\ln \mathcal{Z}^{\rm tot} = \sum_\omega \ln \mathcal{Z}_\omega, \qquad \mathcal{Z}_\omega = \sum_{n=0}^{\infty} z^n \exp\left(-\frac{\beta\hbar\omega n}{1 + \hbar\omega(n-1)/\kappa}\right).$$

Restricting ourselves to MFA ($\beta\kappa \to 0$), the exact expression $\mathcal{Z}_\omega$ is replaced by

$$\mathcal{Z}_\omega^{\rm MFA} = \frac{{\rm e}^{\beta\kappa(\sigma_\omega - 1)}}{1-z}.$$

Here, the mean field $\sigma_\omega = \Lambda(z, \mu_\omega)$ is defined by fugacity z, $\mu_\omega = \hbar\omega/\kappa$, and

$$\Lambda(z, \mu_\omega) \equiv (1-z)\sum_{n=0}^{\infty} \frac{1-\mu_\omega}{1+\mu_\omega(n-1)} z^n.$$

The total energy and pressure of photons in MFA:

$$\mathcal{E}^{\mathrm{MFA}} = \frac{V\kappa^4}{\pi^2(\hbar c)^3}\,\varepsilon_0(z),$$

$$P^{\mathrm{MFA}} = -\frac{\kappa^4}{\pi^2(\hbar c)^3}\left[\frac{T}{3\kappa}\ln(1-z) + \varepsilon_0(z)\right].$$

Monotonic function $\varepsilon_0(z) = \int_0^1 [1-\Lambda(z,\mu)]\mu^2 \mathrm{d}\mu$ ($\varepsilon_0(0) = 0$, $\varepsilon_0(1) = 1/3$) determines the upper bound of energy density (dashed lines), to which the exact value (solid curves) approaches. Besides, $\mathcal{E}^{\mathrm{MFA}} \propto \kappa^4$ at $T \to \infty$, while $\mathcal{E} \propto T^4 \to \infty$ according to the Stefan-Boltzmann law.

The condition $P^{\mathrm{MFA}} = 0$ determines the *threshold temperature*:

$$\frac{T_{\mathrm{thr}}^{\mathrm{MFA}}(z)}{\kappa} = -3\frac{\varepsilon_0(z)}{\ln(1-z)}, \quad \lim_{z\to 0}\frac{T_{\mathrm{thr}}^{\mathrm{MFA}}(z)}{\kappa} = \frac{3}{4}$$

Thus, the presence of $T_{\mathrm{thr}}^{\mathrm{MFA}}$ (and $z < 1$) indicates an additional attraction, requiring energy to overcome it.

Heat capacity $C^{\mathrm{MFA}} = \frac{V}{T^2}\frac{\kappa^5}{\pi^2(\hbar c)^3}\,\eta(z)$, where $\eta(z) \propto z(1-z)$, reflects a zone structure of photon spectrum.

Energy density

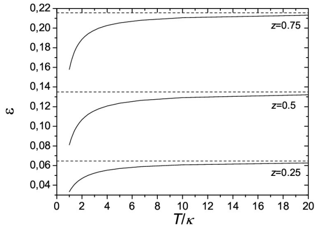

Threshold temperature

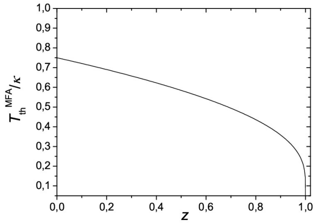

1.3 The role of statistics in an ensemble of extremal black holes

The possibility of compensating the forces of gravitational attraction and electrostatic repulsion in an N-particle system under the condition $eZ = m$ $(G = c = \hbar = 1)$ for the charge eZ and mass m of each particle is reflected in the exact Majumdar–Papapetru solution to the Einstein–Maxwell equations for static and extremal black holes (eBHs) with centers in $\{\mathbf{a}_i \in \mathbb{R}^3\}_{i=1}^N$ for $1.04 \cdot 10^{18}$ GeV $\leq m < M_{\mathrm{Pl}}$ and $1 \leq Z \leq 11$:

$$\mathrm{d}s^2 = -U_N^{-2}(\mathbf{r})\,\mathrm{d}t^2 + U_N^2(\mathbf{r})\,\mathrm{d}\mathbf{r}^2, \quad U_N(\mathbf{r}) = 1 + \sum_{i=1}^{N} \frac{m}{|\mathbf{r} - \mathbf{a}_i|}.$$

Here, the effect of gravitational time delay at the point $\mathbf{r} \in \mathbb{R}^3 \backslash \{B_i\}_{i=1}^N$, B_i is the vicinity of eBH with the event horizon $r_+ = m$, is described by $\mathrm{d}\tau/\mathrm{d}t = U_N^{-1}(\mathbf{r})$, where τ and t are the proper and global times. We estimate (2019) the average time delay σ_d in a statistical ensemble of eBHs with the mean number $\mathcal{N}_d$, which are determined by the fugacity z and the type of statistics d_N (the weight of configurations with N eBHs) as

$$\sigma_d = \mathcal{Z}_d^{-1} \sum_{N=0}^{\infty} d_N z^N \langle U_N^{-1}(\mathbf{r}) \rangle, \quad \mathcal{N}_d = \partial_z \ln \mathcal{Z}_d, \quad \mathcal{Z}_d = \sum_{N=0}^{\infty} d_N z^N.$$

For a uniform eBH distribution without intersections, taking into account the translational invariance of the model and only the points of space allowed for the observer, the dominant contribution to the configurational mean is calculated:

$$\langle U_N^{-1}(\mathbf{r}) \rangle \simeq \frac{1}{1 + \mu N}, \quad \mu = \frac{r_+}{R} < 1,$$

where R is a radius (size) of the system, μ is the model parameter.

In different statistics we compare the value σ_d as a function of the average number $\mathcal{N}$ of eBHs, when a larger time delay appears at smaller values of σ_d.

– Bose-Einstein statistics (BE): $d_N = 1$;

– Infinite statistics (Inf): $d_N = \frac{\Gamma([N/2]+1/2)}{\Gamma(1/2)\,\Gamma([N/2]+1)}$

  Inf looks most likely (A.Strominger, 1993);

– Classical statistics (Cl): $d_N = 1/N!$;

– Fermi-Dirac statistics (FD): $d_N = \frac{g!}{N!\,(g-N)!}$.

One has that 1) $\sigma_{\mathrm{Inf}} > \sigma_{\mathrm{BE}}$ due to repulsion in Inf;
2) $\sigma_{\mathrm{BE}} > \sigma_{\mathrm{Cl}}$, since Cl unphysically enhances the attraction due to the excess number of ensemble replicas;
3) the weakest effect in FD (due to the Pauli exclusion principle) can be established from the approximate functions σ_d, $\mathcal{N}$ for small fugacity z.

Thus, the difference in the time flow can reach $\sim 10\%$ in different statistics, which significantly affects the dynamics of processes in the Universe with the BHs.

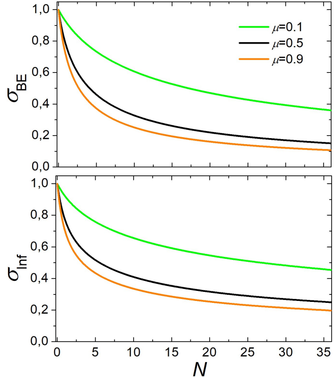

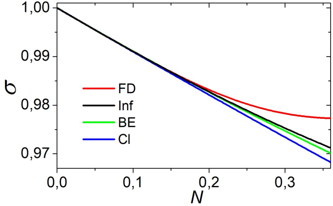

2. Models on manifolds

2.1 The torus universe and spectra of characteristics

To study the time evolution of the geometry of topologically non-trivial spaces (e.g. of extra dimensions), we consider known Riemann surfaces in 2D. Here we consider a torus.

According to (Witten, 1989), (2+1)-gravity is equivalent to the Chern-Simons theory in terms of the triad e^a_μ and the spin connection ω^a_μ. Non-trivial exact solutions arise due to the topology of the space and additional interactions. Let us focus on the action integral on $T^2 = \mathbb{R}^2/\mathbb{Z}^2$ and with the "angular" momentum $I^\mu_a = \mathrm{const}$:

$$S = \frac{1}{2}\int \epsilon^{\mu\nu\lambda} e^a_\mu \left(\partial_\nu \omega_{\lambda a} - \partial_\lambda \omega_{\nu a} + \epsilon_{abc}\omega^b_\nu \omega^c_\lambda\right) \mathrm{d}^3x - \int I^\mu_a \omega^a_\mu \mathrm{d}^3 x,$$

where the metric $g_{\mu\nu} = \eta_{ab} e^a_\mu e^b_\nu$ with $\|\eta_{ab}\| = \mathrm{diag}(-1,1,1)$; $\epsilon_{012} = 1$.

This I^μ_a preserves the curvature form $R_a[\omega] = 0$ and sets the torsion form $T_a = -I^0_a$.

We choose the global variables (u_i, p^i), $i = 1, 2$, and find solutions of field equations using the Dirac's mechanics with constraints combined with the homotopy group.

Here, one has 2 independent abelian holonomies (Wilson loops).

Setting $x^0 = t$ and the gauge-fixing $e^a_0 = \delta^a_0$, $\omega^a_0 = 0$, the solutions are (2004):

$$\omega^a_i = \gamma^a u_i, \qquad e^a_i = \epsilon_{ij} p^j \gamma^a + t E^a_i, \qquad i, j = \overline{1, 2},$$

where terms $E^0_i = \epsilon_{ij} I^j_0$, $E^\alpha_i = -u_i \epsilon^{\alpha\beta}\gamma^\beta - \epsilon_{ij} I^j_\alpha - \epsilon^{\alpha\beta}\gamma^\beta (\epsilon_{ij}/u_j) I^0_0$ and an arbitrary space-like vector γ^a are constant in time t; $\epsilon_{12} = -\epsilon_{21} = 1$.
Given the model constraints, the Dirac bracket defines the Poisson bracket $\{u_i, p^j\} = \delta^j_i$.

▶ Geometrically, the basis vectors of the torus are obtained $\vec{T}_\alpha = (e^\alpha_1, e^\alpha_2)$, linear in t and depended on momentum I^μ_a, what covers the result of (K.Ezawa, 1994).

In (2+1) dimensions, the spectra of "length" L (of space-like intervals), "time" T (of time-like intervals) and area A are of interest. Quantizing, it is required that the states do not depend on the evolution parameter (according to the principle of general relativity), and $L \sim \ell$, $T \sim \tau$ and $A \sim a$, where ℓ, τ and a are the smallest dimensional (Planckian) quantities. However, different quantization schemes can lead to different results, but with a common feature of discreteness/continuity and asymptotics (for macroscopic objects). We show this and a new effect for metrics in conformal form by introducing the generator $J_0 = u_2 p^1 - u_1 p^2$ and the Casimir $Q = \left(u_1 p^1 + u_2 p^2\right)^2$ of $so(2,1)$ (or $su(1,1)$).

- Spectra of characteristics reproduced for $I_a^\mu = 0$ (Freidel, Livine & Rovelli, 2003)
  Interval $\mathrm{d}s_0^2 = Q\left(-\mathrm{d}t^2 + \mathrm{d}\phi^2 + t^2 \mathrm{d}\psi^2\right)$ results in:
  $T_0 = \tau\sqrt{-Q} \mapsto \hat{T}\Psi = \tau\sqrt{n(n-1)}\ \Psi$ (discrete spectrum of "time")
  $L_0 = \ell\sqrt{Q} \mapsto \hat{L}\Psi = \ell\sqrt{s^2 + 1/4}\ \Psi$; (continuous spectrum for $s \in \mathbb{R}$)
  $A_0 = \tau Q \mapsto \hat{A}\Psi = a\tau(s^2 + 1/4)\ \Psi$ (the gap presence due to quantum fluctuations)
- Time level splitting obtained for $I_\alpha^i = \epsilon^{ij}\epsilon_{\alpha\beta} u_j \gamma^\beta h J_0$ (2005)
  The interval $\mathrm{d}s_I^2 = (1 - hJ_0)^2\, \mathrm{d}s_0^2$ and "time" $T_I = (1 - hJ_0)T_0$ determines the spectrum of proper time as a function of parameter $h > 0$:
  $$\hat{T}_I\Psi = \tau\sqrt{n(n-1)}|1 - hm|\ \Psi \text{ for } |m| < n$$
  similarly to the Zeeman effect (for atoms with $so(3)$-spin in external magnetic field)

Thus, the interaction at $m = \pm 1$ either increases $(1+h)T_0$ or decreases $(1-h)T_0$ the time interval compared to the expected T_0, what may depend on the directions of the time-like geodesic (particle) and rotation in the universe.

2.2 Stiefel nonlinear sigma model near two dimensions

The action integral $\mathcal{A}$ and the Lagrangian $\mathcal{L}$ of NLSM in $d = 2 + \varepsilon$ Euclidean dimensions:

$$\mathcal{A} = \frac{1}{2T} \int \mathcal{L} \, \mathrm{d}^d x, \quad \mathcal{L} = \mathrm{Tr}\left(\boldsymbol{\nabla} U^\top \mathrm{g} \boldsymbol{\nabla} U\right), \quad \mathrm{g}(U; \lambda) = I_N + (\lambda - 1) U U^\top,$$

where the temperature T, $N \times k$-matrix field $U(x) \in SO(N)/SO(N-k)$, $U^\top U = I_k$, gradient $\boldsymbol{\nabla} = (\partial/\partial x_1, \ldots, \partial/\partial x_d)$, and parameter (of the metric anisotropy) $\lambda > 0$.

Geometric properties are encoded in Christoffel function of the second kind (Hüper, 2021),

$$\Gamma(\xi, \eta) = \frac{1}{2} U \left(\xi^\top \eta + \eta^\top \xi\right) + (1 - \lambda) \Pi \left(\xi \eta^\top + \eta \xi^\top\right) U; \qquad \Pi = I_N - U U^\top,$$

and the curvature $(1,3)$-tensor for tangent vectors $\xi, \eta, \phi \in \mathcal{TM}$ (D.Nguyen, 2022)

$$R(\xi, \eta)\phi = \mathrm{D}_\eta \Gamma(\xi, \phi) - \mathrm{D}_\xi \Gamma(\eta, \phi) + \Gamma(\eta, \Gamma(\xi, \phi)) - \Gamma(\xi, \Gamma(\eta, \phi)),$$

where the derivative D_ξ in the direction ξ at the point U is involved.

Using the background field method, we represent $U = U_0 + V - (1/2)\Gamma(V, V) - \ldots$ in terms of the slow field U_0 and *normal* (fast) coordinates V to get $U^\top U = U_0^\top U_0 = I_k$.

In the 1-loop approximation, we restrict ourselves to the Lagrangian quadratic in V:

$$\mathcal{L}[U] = \mathcal{L}[U_0] + 2\mathrm{Tr}(\boldsymbol{\nabla} U_0^\top \mathrm{g}_0 \widehat{\boldsymbol{\nabla}} V) + \mathrm{Tr}[(\widehat{\boldsymbol{\nabla}} V)^\top \mathrm{g}_0 \widehat{\boldsymbol{\nabla}} V] - \widetilde{K}(\boldsymbol{\nabla} U_0, V),$$

where the covariant derivative $\widehat{\boldsymbol{\nabla}} V = \boldsymbol{\nabla} V + \Gamma(V, \boldsymbol{\nabla} U_0)$ and the biquadratic $(0,4)$-form $\widetilde{K}(\xi, \eta) = \mathrm{Tr}[\eta^\top \mathrm{g} R(\xi, \eta)\xi]$ (G.Jensen, 1975) are taken in the metric $\mathrm{g} = \mathrm{g}_0 \equiv \mathrm{g}(U_0; \lambda)$.

We renormalize $\mathrm{g} = \mathrm{g}(U; \lambda)$ (2024) by adding the covariant counterterms h to the bare metric $\mathrm{g}_0 = \mathrm{g}(U_0; \lambda)$ and expanding in $\varepsilon = d - 2$ for the scale μ:

$$\mathrm{g} = \mu^\varepsilon \mathrm{g}_0 + \mathrm{h}.$$

Quantum averaging over V results in the IR divergence at $\varepsilon \to 0$: $\langle\!\langle \widetilde{K}(\boldsymbol{\nabla} U_0, V)\rangle\!\rangle = \mathrm{Ric}(\boldsymbol{\nabla} U_0, \boldsymbol{\nabla} U_0)\,\Delta(0)$, where

$$\Delta(0) = T\frac{\Omega_{d-1}}{(2\pi)^d}\int_\mu k^{d-3}\mathrm{d}k = -\frac{T}{2\pi\varepsilon} - \frac{T}{2\pi}\ln\mu + O(\varepsilon).$$

Eliminating ε^{-1}-terms using the scaling factors Z's for $t = T/(2\pi)$ and $\tau = t/\lambda$ at the metric components, one gets beta-functions $\beta_t = \mathrm{d}t/\mathrm{d}s$, $\beta_\tau = \mathrm{d}\tau/\mathrm{d}s$ for $s = \ln\mu$:

$$\beta_t = \varepsilon t - [N-2-\lambda(k-1)]t^2,$$

$$\beta_\tau = \varepsilon\tau - \left[\lambda^2(N-k) + \frac{k-2}{4}\right]\tau^2,$$

determined by the Ricci tensor components in [...].
Given $\beta_\lambda = \mathrm{d}\lambda/\mathrm{d}s$ by using $\beta_\lambda/\lambda = \beta_t/t - \beta_\tau/\tau$, one has the **sink** $(\lambda_-; t_-)$ and the **saddle point** $(\lambda_+; t_+)$;

$$\lambda_\pm = \frac{N-2}{2(N-1)}\left[1 \pm \sqrt{1 - \frac{(k-2)(N-1)}{(N-2)^2}}\right],$$

$$t_\pm = \frac{\varepsilon}{N-2-\lambda_\pm(k-1)}.$$

For $d > 2$ and $2 < k < N$, the sink ●, at which 4 phases meet, seems tetracritical (expected to appear in super-conductivity with Anderson (de)localization).
At $k = 2$ and $d > 2$, the sink ● becomes bicritical point.

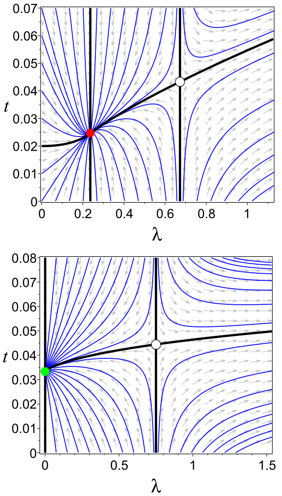

RG trajectories and velocity field

Top: $N = 12$, $k = 9$, $d = 2.2$

Bottom: $N = 5$, $k = 2$, $d = 2.1$

Vertical lines - Einsteinian spaces

3. Models of Bose-condensate dark matter

3.1 Dense and dilute phases of DM

To improve the description of the observables (rotational curves, etc.), we replace models with pair interaction in the Thomas–Fermi approximation (T.Harko; P.Chavanis et al) by models with quantum fluctuations and multiparticle self-interaction $V_{\rm SI}$, but without flows (it means that the condensate wave function ψ is real, and ψ^2 is the particle density):

- $V_{\rm SI} = \frac{U}{3}\psi^6$ (2020): DM halo model "core (2 phases)+tail"; "right" scaling of the mass-radius ratio
- $V_{\rm SI} = \frac{U_2}{2}\psi^4 + \frac{U_3}{3}\psi^6$ (2021): dominating rarefied phase in M81-galaxy
- $V_{\rm SI} = \frac{U}{v}[1-\cos(\sqrt{v}\psi)] - \frac{U}{2}\psi^2 = U\left[-\frac{v}{4!}\psi^4 + \frac{v^2}{6!}\psi^6 - \ldots\right]$ (axionlike SI) (2023)

for central regions of spherical DM halo with relatively high particle density

The starting point is the extremization of the (free-energy) functional F by taking into account the Poisson equation $\Delta_r V_{\rm gr} = 4\pi G m\psi^2$ for $m \simeq 10^{-22}$ eV$/c^2$:

$$F = 4\pi\int_0^R \left[\frac{\hbar^2}{2m}(\partial_r\psi)^2 - \mu\psi^2 + mV_{\rm gr}\psi^2 + V_{\rm SI}\right] r^2\,\mathrm{d}r$$

Here we focus on the model with (2+3)-particle SI, which evolves spatially in terms of dim-less quantities $\chi = \sqrt{m/\rho_0}\psi$, $\xi = r/r_0$ as

$$\frac{1}{2}\Delta_\xi\chi + u\chi - A\chi\varphi - Q\chi^3 - B\chi^5 = 0, \quad \Delta_\xi\varphi = \chi^2,$$

where Δ_ξ is the radial part of Laplace operator.

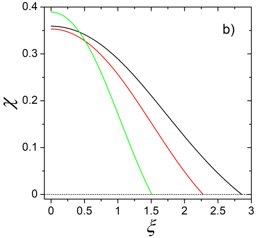

$A = 10,\ B = 20,\ Q = 1.36$
$u_{\rm black} \simeq 0.149,$
$u_{\rm red} \simeq -0.502,$
$u_{\rm green} \simeq -2.046$

Defining the chemical potential $\mu(\xi)$, which involves the gravitational potential and quantum fluctuations, and using the Gibbs–Duhem and Euler relations, we obtain the particle density σ, internal pressure P and internal energy E based on the solution $\chi(\xi)$ parametrized by u at $T = 0$:

$$\sigma = \frac{3}{\xi_B^3}\int_0^{\xi_B} \chi^2(\xi)\,\xi^2 \mathrm{d}\xi,$$

$$P = \frac{3}{\xi_B^3}\int_0^{\xi_B} p(\xi)\,\xi^2\,\mathrm{d}\xi, \quad p(\xi) = \frac{Q}{2}\chi^4(\xi) + \frac{2}{3}B\chi^6(\xi),$$

$$E = \int_0^{\xi_B} \varepsilon(\xi)\,\xi^2\,\mathrm{d}\xi, \qquad \varepsilon(\xi) = \frac{Q}{2}\chi^4(\xi) + \frac{1}{3}B\chi^6(\xi).$$

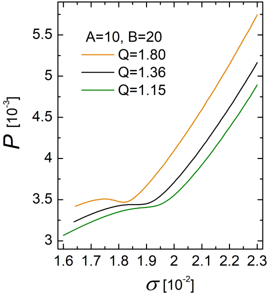

For galactic DM cores with a central mass density $\rho_0 \simeq 10^{-20}\ \mathrm{kg\,m^{-3}}$ and radius $\lesssim 1$ kpc, we take the measure of gravitational interaction $A \sim 10$ to estimate r_0:

$$r_0 \simeq 0.824\ \mathrm{kpc}\left[\frac{A}{10}\right]^{1/4}\left[\frac{mc^2}{10^{-22}\ \mathrm{eV}}\right]^{-1/2}\left[\frac{\rho_0}{10^{-20}\ \mathrm{kg\,m^{-3}}}\right]^{-1/4}.$$

The characteristic energy density is evaluated as

$$\varepsilon_0 \simeq 33.82\ \mathrm{eV\,cm^{-3}}\left[\frac{A}{10}\right]^{-1/2}\left[\frac{mc^2}{10^{-22}\ \mathrm{eV}}\right]^{-1}\left[\frac{\rho_0}{10^{-20}\ \mathrm{kg\,m^{-3}}}\right]^{3/2}.$$

In the pressure units, $33.82\ \mathrm{eV\,cm^{-3}} \simeq 5.42\times10^{-12}\ \mathrm{Pa}$.

3.2 Two-axion composite (dimer) and Feshbach resonance

- When a bound state has $E \sim 0$, how to pass a particle (p2) with $E \sim 0$ through a domain wall? $\Rightarrow$ Apply two channels $(1,2)$ + resonance transition between them $\Rightarrow$ the Feshbach resonance concept:
- The appearance of a dimer with $E > 0$ & finite lifetime is detected due to resonant scattering in an open channel (2)
- The scattering length a varies in an infinite range (Feshbach phenomenon)

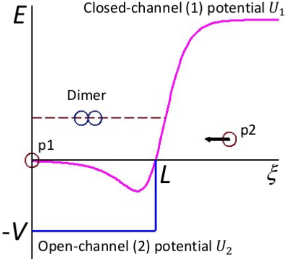

Resonance zone: $\xi \in [0; L]$

Two-channel QM is given by stationary coupled Schrödinger eqs with Hamiltonians $H_{1,2} = -\partial_\xi^2 + U_{1,2}(\xi)$ determining $\chi^{(1)}$ and $\chi^{(2)}$ for the closed and open channels:

$$\begin{aligned}(H_1 + Q - E)\chi^{(1)} + \Omega\chi^{(2)} &= 0,\\ (H_2 - E)\chi^{(2)} + \Omega^\dagger\chi^{(1)} &= 0,\end{aligned}$$

where $Q = E^{(2)} - E^{(1)}$ is an energy gap at $\Omega = 0$ (when E is 2-degenerated). Energy level E splits under action of "external impact":

$$\Omega(\xi) = -\omega^2\,\theta(L-\xi), \qquad \Omega^\dagger = \Omega.$$

Model parameters are V (potential), ω^2 (impact), Q (gap), L (resonance zone width).

The unperturbed solutions: $H_1\chi_{\rm ak}(\xi) = 0 \;\rightarrow\; \chi_{\rm ak}(\xi) = 4\arctan\exp(L-\xi)$ (antikink)

$$(H_2 - E)\tau_0 = 0 \;\rightarrow\; \tau_0(\xi) = \sin K\xi,\; K = \sqrt{E+V}$$

Solution in the first approximation (and 1d):

$$\chi^{(1)}(\xi) = \frac{\lambda}{N(L)} \langle \xi | \chi_{\rm ak} \rangle,$$

$$\chi^{(2)}_{<}(\xi) = \tau_0(\xi) - \frac{\lambda}{N(L)} \langle \xi | G_2^{(+)} \Omega^\dagger | \chi_{\rm ak} \rangle,$$

$$\chi^{(2)}_{>}(\xi) = A \sin(k\xi + \delta),$$

where the normalization $N(L) = \langle \chi_{\rm ak} | \chi_{\rm ak} \rangle$; $G_2^{(+)} = (H_2 - E - {\rm i}\epsilon)^{-1}$, $k = \sqrt{E}$.

We extract info on dimer from the phase shift δ.

Multiplier λ indicates the "dressed" state:

$$\lambda = \frac{\langle \chi_{\rm ak} | \Omega | \tau_0 \rangle}{E - Q + N^{-1}(L) \langle \chi_{\rm ak} | \Omega G_2^{(+)} \Omega^\dagger | \chi_{\rm ak} \rangle} = \frac{\langle \chi_{\rm ak} | \Omega | \tau_0 \rangle}{E - Q + \omega^4 \Delta_L(K) + {\rm i}\omega^4 \gamma_L(K)}$$

Scattering length $a(\omega^2)$ at $E \to 0^-$ determines the dimer 1d-wave-function $\propto \exp(-\xi/a)$ and the binding energy $E_{\rm bind} \simeq -1/a^2$ for $a \gg L$.

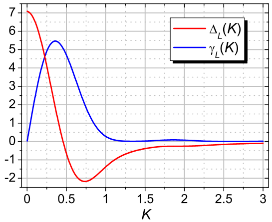

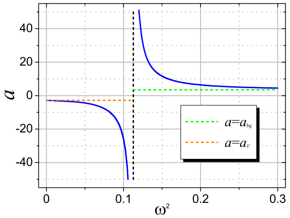

Resonance zone: $\xi \in [0; L]$

$$a(\omega^2) = a_{\rm bg} \left(1 + \frac{\alpha \omega_c^4}{\omega^4 - \omega_c^4} \right)$$

leads to the diversity of a in galaxies

At $k \neq 0$, a pole $E_{\rm res} = E_0 - \mathrm{i}\Gamma_0/2$ of S-matrix (its element) is found from the equation:

$$K^2 = V + Q - \omega^4 \left[\Delta_L(K) + \mathrm{i}\gamma_L(K) \, \frac{k \cot KL - \mathrm{i}K}{K \cot KL - \mathrm{i}k} \right],$$

where $k = \sqrt{K^2 - V}$ and $E = K^2 - V$.

We numerically obtain $E_0 \simeq 0.175$ and $\Gamma_0 \simeq 0.148$, as well as $\sqrt{E_{\rm res}} = k_{\rm res} - \mathrm{i}æ_{\rm res}$ with $k_{\rm res} \simeq 0.427$.

The phase shift near the resonance is

$$\delta(k) = \delta_0 - \arctan \frac{æ_{\rm res}}{k - k_{\rm res}},$$

$$\delta(k_{\rm res} - 0) - \delta(k_{\rm res} + 0) = \pi.$$

The cross-section (from the optic theorem in 1d):

$$\sigma(k) = 2 \sin^2 \delta(k).$$

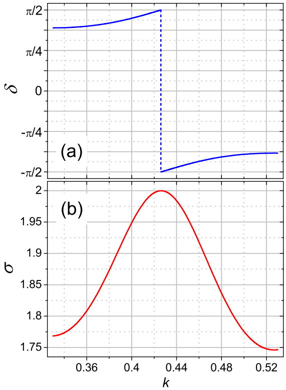

$L = 5,\ Q = 0.15,\ \sqrt{V} = 0.2$

For a typical time scale $\tau = m r_0^2/\hbar \simeq 9.7 \cdot 10^5$ yrs for ultralight DM in (dwarf) galaxies, the lifetime of the dimer is being (2023)

$$t_{\rm D} = \frac{2\tau}{\Gamma_0} \simeq 1.313 \cdot 10^7 \text{ yrs}$$

This allows dimers' participation in the formation of large-scale DM structures. The question arises about the internal degrees of freedom of DM particles that lead to two-channel scattering.

Summary

1. It is shown that quark-gluon matter can provide, under ADD conditions, a non-zero probability of manifestation of extra dimensions, whose number is <6 in the confinement regime and unlimited, but determined by temperature, in the radiation-dominated regime.
2. Given the law of addition of 4-momenta with the Planck upper bound, thermodynamic functions and modified Stefan-Boltzmann law of black body radiation are found. We show that radiation occurs at temperatures above the threshold and with a limited energy density.
3. For an ensemble of extremal black holes described by the static Majumdar–Papapetrou solution to the Einstein–Maxwell equations, the average value of the gravitational time delay differs in Bose–Einstein, infinite, Fermi–Dirac, and classical statistics.
4. Using the Hamiltonian approach, it is described the time evolution of the geometry of torus space in (2+1)-dimensional Chern-Simons gravity with a model source, whose presence, upon quantization, leads to the splitting of degenerate states of proper time.
5. Focusing on the $(2+\varepsilon)$-dim NLSM on a real Stiefel manifold, the background-field method and normal coordinates are used for the quantum consideration and a RG description in terms of 2 effective charges to reveal tetracriticality in physics.
6. Having obtained solutions to the stationary Gross–Pitaevskii equation with gravitational and nonlinear self-actions, as well as thermodynamic functions, dense and dilute states of dark matter (DM) and the first-order phase transition between them are revealed.
7. Based on the Feshbach resonance, the mechanism of formation of long-lived dimers, which can participate in the formation of large-scale DM structures, is elucidated. The same mechanism explains the scattering length variety.

THANK YOU FOR ATTENTION!

Selected publications

Strong interacting matter

[1] A.V. Nazarenko. Relativistic direct interaction between nucleons derived from classical field theory. *Int. J. Mod. Phys. E* **13**(3), 631–645 (2004).
[2] A.V. Nazarenko. Superfluidity in a system of neutrons with direct relativistic interaction. *Ukr. J. Phys.* **50**(3), 293–298 (2005).
[3] A.V. Nazarenko. Evaporation of symmetric nuclear matter in weakly curved space. *Int. J. Mod. Phys. E* **15**(3), 561–570 (2006).
[4] D.V. Anchishkin and A.V. Nazarenko. Liquid-like phases of $\pi^+\pi^-$ matter. *J. Phys. Stud.* **10**(2), 93–97 (2006).
[5] M. Gyulassy, Iu.A. Karpenko, A.V. Nazarenko, and Yu.M. Sinyukov. HBT and initial conditions for hydrodynamic expansion in A+A collisions. *Braz. J. Phys.* **27**(3a), 1031–1038 (2007).
[6] Yu.M. Sinyukov, Iu.A. Karpenko, and A.V. Nazarenko. Spacetime scales and initial conditions in relativistic A+A collisions. *J. Phys. G: Nucl. Part. Phys.* **35**, 104071 (5 pages) (2008).

Models on manifolds

[1] A.V. Nazarenko. Directed random walk on the lattices of genus two. *Int. J. Mod. Phys. B* **25**(26), 3415–3433 (2011).
[2] A.V. Nazarenko. Area quantization of the parameter space of Riemann surfaces in genus two. *Ukr. J. Phys.* **58**(11), 1055–1064 (2013).
[3] A.V. Nazarenko and V. Blavatska. A one-dimensional random walk in a multi-zone environment. *J. Phys. A: Math. Theor.* **50**, 185002 (11 pages) (2017).
[4] A.A. Nazarenko, A.V. Nazarenko. Structures associated with the Borromean rings' complement in the Poincaré ball. *Ukr. J. Phys.* **69**, 498-514 (2024).
[5] A.M. Gavrilik, A.V. Nazarenko. Scaling behavior and phases of nonlinear sigma model on real Stiefel manifolds near two dimensions. arXiv:2412.02472

Gravitating systems

[1] A.V. Nazarenko. Classical relativistic system of pointlike masses with linearized gravitational interaction. *Acta Phys. Slovaca* **53**(1), 1–16 (2003).
[2] A. Nazarenko. Thermodynamic functions of a relativistic system of charges in the ring-diagram approximation. *Ukr. J. Phys.* **49**(2), 182–187 (2004).
[3] A. Nazarenko. Time level splitting in quantum Chern–Simons gravity. *Class. Quantum Grav.* **22**, 2107–2120 (2005).
[4] A.V. Nazarenko. The probability of the creation of extra dimensions in nuclear collisions. *Int. J. Mod. Phys. E* **17**(8), 1605–1618 (2008).
[5] W.S. Chung, A.M. Gavrilik, and A.V. Nazarenko. Photon gas at the Planck scale within the doubly special relativity. *Physica A* **533**, 121928 (10 pages) (2019).
[6] A.M. Gavrilik and A.V. Nazarenko. Statistics effects in extremal black holes ensemble. *Int. J. Mod. Phys. A* **34**, 1950215 (16 pages) (2019).

Dark matter models

[1] A.M. Gavrilik, I.I. Kachurik, M.V. Khelashvili, and A.V. Nazarenko. Condensate of μ-Bose gas as a model of dark matter. *Physica A* **506**, 835–843 (2018).
[2] A.V. Nazarenko. Partition function of the Bose–Einstein condensate dark matter and the modified Gross–Pitaevskii equation. *Int. J. Mod. Phys. D* **29**(2), 2050018 (18 pages) (2020).
[3] A.M. Gavrilik, M.V. Khelashvili, and A.V. Nazarenko. Bose–Einstein condensate dark matter model with three-particle interaction and two-phase structure. *Phys. Rev. D* **102**(8), 083510 (13 pages) (2020).
[4] A.M. Gavrilik and A.V. Nazarenko. Phases of the Bose–Einstein condensate dark matter model with both two- and three-particle interactions. *Universe* **7**, 359 (11 pages) (2021).
[5] A.M. Gavrilik, I.I. Kachurik, A.V. Nazarenko. New deformed Heisenberg algebra from the μ-deformed model of dark matter. *Front. Astron. Space Sci.* **10**, 1133976 (10 pages) (2023).
[6] A.M. Gavrilik and A.V. Nazarenko. Axionlike dark matter model involving two-phase structure and two-particle composites. *Phys. Rev. D* **108**, 123030 (17 pages) (2023).